Available online at www.sciencedirect.com
SCIENCE DIRECT®
International Journal of Heat and Fluid Flow 25 (2004) 833–840
International Journal of HEAT AND FLUID FLOW
www.elsevier.com/locate/ijhff

Supersonic liquid fuel jets injected into quiescent air

S. Zakrzewski, B.E. Milton *, K. Pianthong, M. Behnia

School of Mechanical and Manufacturing Engineering, University of New South Wales, Sydney NSW 2052, Australia

Received 14 January 2004; accepted 16 May 2004

Abstract

Supersonic fuel jets may have applications in diesel engine and scramjet technology. Their properties require a fundamental examination as their mixing characteristics are likely to be affected by the leading edge shock wave. Such jets have been created experimentally in the laboratory but require further CFD studies to examine details that are obscure in the experiments. This paper reports on the CFD methods used. These include a solid body assessment of the formation of the leading edge shock, the steady state and transient analysis of the mixing layer in supersonic vapour and liquid jets. A liquid jet, transient solution is computationally expensive even when atomization and vaporization are not included. Some typical results are outlined.

1. Introduction

Supersonic liquid jets have many technological and scientific applications such as material cutting, cleaning, mining and tunneling. Hence, during the past few decades, a number of investigators have studied the generation and characteristics of high-speed water jets. These include both continuous and intermittent, pulsed jets. In these applications, jet coherence is more important than its atomization and mixing. Recently, high-speed, pulsed liquid jets in the high subsonic range, have been considered for the improvement of atomization and combustion in diesel engines. Injection pressures of up to 230 MPa have been reached. Using special equipment, even higher speed jets in the supersonic range are possible. These need fundamental studies both for the purpose of diesel engine combustion and for another potential application, scramjet engines, where the combustion must occur in the supersonic jet stream within the extremely short residence time in the combustion chamber.

With all high velocity fuel jets, the important factors are improved combustion efficiency and smoke reduction. A noticeable difference between supersonic and subsonic jets is the development of a leading edge shock wave in the former that modifies both the air/liquid mixing and the temperature distribution from the leading edge of the jet. The increased turbulent mixing and improved atomization is a basic factor in smoke reduction while the higher shock induced temperature can decrease the ignition delay. Fundamental studies, for example those of Field and Lesser (1977), Shi and Takayama (1995, 1999), Nakahira et al. (1991) have shown that the shock wave effect is significant.

In the present work, jet velocities in the range 600–2400 m/s have been obtained experimentally. The jet is an intermittent, single event lasting for less than a millisecond. Measurements within the jet are extremely difficult. The use of CFD is advantageous as experimental studies are unable to capture many of the details and are intrusive. However, even CFD presents many difficulties. In the present work, the approach used to solve this problem and some results are considered. The CFD studies to date have been pre-dominantly confined to the lower end of the above supersonic velocity range.

The aim of the work presented here is to develop a computational scheme based on commercial CFD codes that will help to provide information on the mixing characteristics of these jets. Code validation is difficult. In this work, experimental flow visualisation of the shock wave structures and the jet shape has been used for this purpose. At this stage, the simulation has been

* Corresponding author. Tel.: +61-2-9385-5699; fax: +61-2-9663-1222.
E-mail address: b.milton@unsw.edu.au (B.E. Milton).

0142-727X/$ - see front matter © 2004 Elsevier Inc. All rights reserved.
doi:10.1016/j.ijheatfluidflow.2004.05.010

for water jets in the low supersonic range (e.g. $M = 1.8$) although extension of the work to higher jet velocities and other fluids is envisaged.

2. Experiments with intermittent supersonic liquid jets

The high-speed, pulsed liquid jets were generated using the momentum exchange from the impact of a high velocity projectile on the liquid contained in the nozzle sac, as described by Pianthong et al. (2003). The liquid was ejected to the atmospheric air through the short, parallel nozzle. Various shapes were used for the sac/nozzle approach combination, the most common being a short cylindrical sac of the same diameter as the projectile followed by a conical contraction of about 40° included angle to the nozzle. Two jet velocity ranges were explored, these being a low value of approximately 400–600 m/s and a high range, 1800–2400 m/s. The polycarbonate projectile was launched from a vertical, downward firing powder gun with a velocity of 325–1100 m/s depending on the velocity range under investigation. Sufficient propellant was required in the cartridge for good repeatability; too little propellant leading to inconsistent results due to unburned residues. The liquid/projectile mass ratio and exit orifice diameter (d) are important in determining this design. For the low jet velocities, 0.25 g of propellant and a 5 mm diameter nozzle were used while for the high velocities, the equivalent values were 0.83 g and 0.5–1 mm diameter respectively. Visualisation was undertaken using a shadowgraph apparatus. The trigger signal for the argon light source was provided by a pressure transducer with the region of interest being captured by high-speed 3000ASA Polaroid film with an effective photographic area of 90×120 mm.

It is known that a solid body travelling at supersonic speed produces a shock wave ahead of the body in the medium in which it is travelling and a similar phenomenon occurs with a liquid jet. This is shown from experiments as illustrated in Figs. 1 and 2 for jets of 620 m/s ($M = 1.8$) and 1800 m/s ($M = 5.2$) respectively.

As an assumed jet shape is important in predicting a realistic shock location and shape by CFD, experimental, high resolution, liquid jet photographs were used to review the jet shape. Both water and diesel fuel was used in the experiments reported by Pianthong et al. (2002, 2003). For the 600 m/s ($M = 1.8$) jets, the profile develops from a flat front to a rounded bow within some 10 mm. This shape is reasonably consistent with that obtained for jets at high subsonic velocities from single hole nozzles, the major difference being the appearance of the detached bow shock wave. Surface instabilities and ligaments appear during this profile transition period. At the high velocity of 1800 m/s ($M = 5.2$), the bow

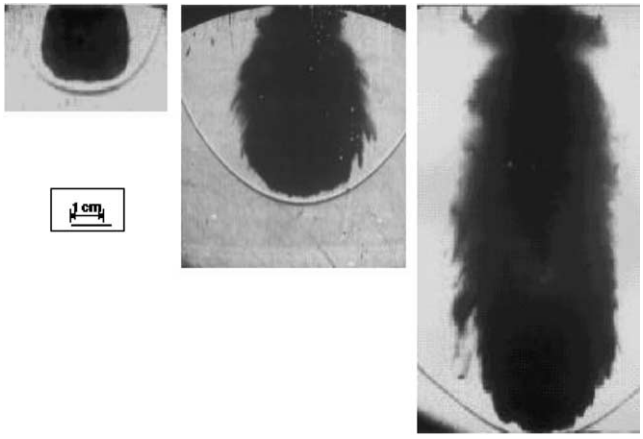

Fig. 1. Water jet and shock wave at $M = 1.8$ (620 m/s) showing the jet development and detached bow shock wave.

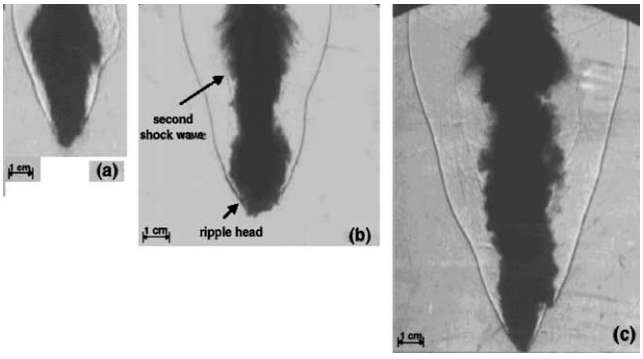

Fig. 2. Diesel fuel jet and shock wave at $M = 5.2$ (1800 m/s) showing the jet development, oblique bow shock and secondary shock waves.

shape is more pointed and shows signs of an oscillation from more to less pointed. The bow shock is now attached and is instrumental in this altered appearance. Secondary shocks are discernible from at least one and, as the jet lengthens, at two locations on its side. A one-dimensional analysis of the driving processes within the nozzle sac, highlights the importance of a second shock wave system within the liquid in the nozzle that reflects backwards and forwards raising the driving pressure to very high values, greater than 4 GPa. This explains the jet pulsing and secondary external shock wave system for the $M = 5.2$ case found in the air surrounding the emerging jet. The lower speed jet does not exhibit this behaviour. The analysis indicates that, for the lower projectile impact velocity in this latter case, the wave motion in the liquid remains subsonic (for example, with a maximum velocity of around 1700 m/s compared with the local sound speed of about 1800 m/s) and the wave reinforcing process in the nozzle sac is consequently smeared. Typically, the total jet efflux times for the 8 mm diameter, 10 mm long nozzle sac are from 1 ms (600 m/s jet) down to 250 μs (2400 m/s jet).

3. Modelling supersonic liquid jets

The lower speed jets in the above range are more likely to have immediate practical applications, and hence the higher velocities where the shock becomes attached are not the prime targets of the present paper. Only the $M = 1.8$ (600 m/s) range has been considered for CFD analysis at this stage. Also, in the simulations, the jet was assumed to be water or water vapour, not diesel fuel as the latter is a complex mixture of many components and its properties are not as clearly defined. Note that the differences exhibited between the two fluids, water and diesel fuel in the flow visualisation (shock wave shapes, jet profiles) as shown on Fig. 2 are small although other characteristics such as jet attenuation which are not as relevant to the present paper, are more marked.

It is extremely difficult to determine experimentally such things as the boundaries of the liquid core of the jet, the porous mixing layers where air is entrained into the liquid and the outer droplet shroud. Thus, a simulation to help understand the jet structure is important. The current simulation uses the proprietary code, FLUENT. In modelling such a complex process as a transient, supersonic deformable surface, several factors need to be considered. In particular, these are the shock wave formation ahead of the jet and the density variations from the surrounding air, through the mixing layer to the liquid core. While several turbulence approaches were examined, the k–ε model was found to provide the only suitable solution due to convergence problems with the others.

3.1. Shock wave structures ahead of the jet

The first consideration is whether the shock wave system can be predicted with reasonable accuracy. For steady flow and a solid body, this is a straightforward application of the code. From an initial calibration against a sphere reported by Zakrzewski et al. (2002) where ample experimental data is available, good agreement was found in the bow shock wave shape and stand-off distance. For the jet of Mach number 1.8, the jet geometry was first chosen as a solid body with a profile determined from the corresponding experiments. This is shown on Fig. 3. The predicted and experimental shock wave density profiles are illustrated on Fig. 4. Contours between the shock wave and jet show the increasing density as the flow behind the shock wave slows further. The comparison shows that the shock stand-off is slightly over-predicted but is in an acceptable range. One reason is that the placement of the jet head in the experiment is somewhat ambiguous due to the surrounding vapour and droplet cloud. This means that the actual interface between the liquid and the gas is open to interpretation. If it is slightly further back towards the nozzle, then the agreement improves. Two other reasons for the difference are firstly, the computational results are for a steady state solution whereas in reality the jet is growing. The shock is therefore a transient phenomenon, which is evolving as the jet geometry changes. The second is that the interface between the liquid and the gas is not a solid wall. As the liquid jet is atomized, the core becomes increasingly porous so that some airflow diffuses into the quasi-porous medium. The head is still locally supersonic so the shock still propagates. Ben-Dor et al. (1997) suggest that the bow shock wave in front of porous materials quickly attenuates. Hence, the resultant shock will move towards the body. Incorporation of a cavity, that is, a sudden reduction in jet cross-section behind the jet head as suggested by Bloor (1978) provided only marginal

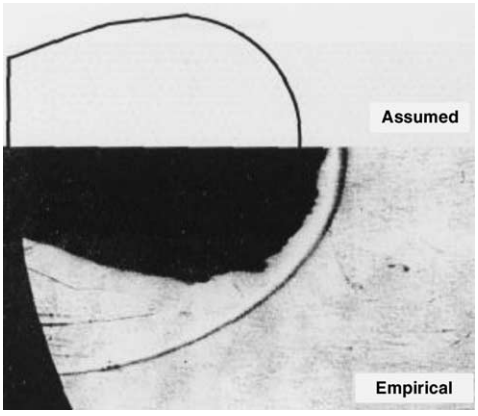

Fig. 3. Solid body profile used in the simulation.

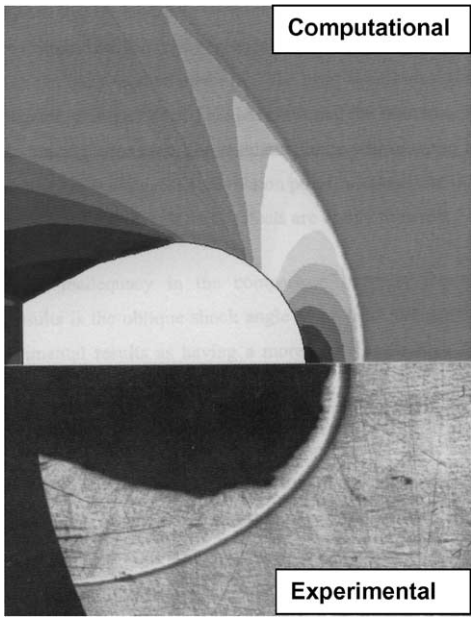

Fig. 4. Comparison of experimental shock location with the simulation.

improvement. It is therefore believed that the simulation differences are due to the reasons given above. As these effects have not been simulated, the present comparison is quite reasonable.

3.2. The jet mixing layer solution

The aspect of high-speed liquid jets now considered is their transient nature, the effect the shock has on the jet head and the properties of the bow shock wave ahead of the jet. This is undertaken with the use of the species transport equations in FLUENT to predict the transient development of the jet. The mass concentrations in the mixing region used a species (O_2, N_2, H_2O) convection-diffusion equation with the properties of water, as these are well defined compared to fuels although both water and fuel jets were examined experimentally. The method uses the FLUENT models for jet break-up that does not give atomisation details but indicates the mass fraction of each species at each location.

Previous work, for example that of Reitz and Bracco (1982) and Lian and Reitz (1993) on subsonic jets has considered the instabilities in a jet, their effect upon the atomization process and the pressure distribution in the jet, and has predicted droplet size and distribution. The most pertinent to the present study is the work of Bloor (1978) who incorporated the numerical equations for supersonic flow into the computational solver, splitting the physical phenomena into a numerical domain constructed of layers, each being dependent on their respective boundary conditions. Resnyansky et al. (1997) investigated the shock wave propagation in a one-dimensional, unsteady, two-phase flow. This method does not, as such, predict atomization but generates a local mass fraction for the mixing layers that can describe mixing dependent phenomena.

The methodology now used is as follows. First, the ability of the numerical code to solve supersonic multiphase flows was studied with emerging jets as either vapour or liquid. This was initially a steady state solution to illustrate core jet formation and mixing layer interactions. The governing equations in their unsteady form were then solved. The density effect was also examined by modification of the code allowing species dependent densities to be set. While detailed comparison with the core jet from experiment was not possible, the transient numerical approach was tested by comparison against the jet shape and position over its life span from experiment. In the simulations, the assumptions made were that:

- the jet is axi-symmetric.
- the liquid inlet boundary has a constant mass flow.
- the liquid and gas are immiscible.
- the liquid is incompressible.
- the gas is compressible, obeying the ideal gas law.
- the density ratio gives a species mass fraction concentration in the mixing layer.

3.2.1. The supersonic vapour jet

As one of the experimental liquids is water, the simulation assumes injected water vapour with density 0.55 $kg\,m^{-3}$. The air consists of oxygen (O_2) and nitrogen (N_2) with a mass fraction of 0.23 and 0.77 respectively. The solver computes for the three species, each having its own diffusion coefficient for predicting the interactive behaviour with other species. All the species are assumed to obey the ideal gas law. This is somewhat of an assumption for early stages of injection but allows the solver to use a global density model. That is, it is assumed that the liquid is instantaneously atomized and then vaporized.

3.2.2. The supersonic liquid jet

The simulation of the liquid jet discussed in this section is an extended approach to the computational modelling of Section 3.2.1, the difference being the high density ratios and their governing relationships between the multi-species flows. Because the density ratio of liquid to air is about 1000:1, a further high gradient has to be resolved in the numerical scheme.

In the vapour jet calculations, the computational model used the assumption, unrealistically, that all species, including those in the mixing region followed the same density law. The default settings for FLUENT is that the density law for each species can only be set to either a constant value or an ideal gas or quasi-ideal gas and each species has to obey the same law. The code may be modified by the addition of compiled Used Defined Functions (UDF). This provides the ability to solve with an individual density law for each species. However, it adds considerably to the numerical stiffness and the additional computational time is extensive. The UDF assumptions made here are that the liquid has a constant density; the gas follows the ideal gas law density and the mixture is controlled by a volume-weighted law.

The solver stability, decreased by the inclusion of the UDF function, means that a steady state solution cannot be achieved immediately with initialisation at the desired boundary conditions. Divergence occurs rapidly. A high node-density grid and a pre-solution adaptive technique is then necessary to progressively generate a result. The latter is carried out by gaining a converged solution in numerically stable conditions, that is by gradually increasing the density ratio between liquid and gas from a low value of near 1. The data from one calculation is used for the initialisation of the next. This quasi-iterative scheme guarantees numerical stability whilst still giving convergence at the desired conditions. A draw back of this method is that it is computationally expensive although less than the high node-density mesh.

The unsteady calculations for a high-speed liquid jet incorporate all the above. The pre-solution adaptive technique cannot be instigated in the unsteady numerical procedure, so the high node-density mesh is utilized instead. The major difference in the results compared to those for the vapour jet is in the density profiles since there is no density fluctuation in the core jet and the liquid density in the mixing layer is not pressure dependent. However, a shock is now shown to occur.

4. Simulation results for the mixing layer

4.1. The vapour jet

4.1.1. Steady state calculations

The profile of a water vapour jet issuing out of the 5 mm diameter nozzle at approximately Mach 1.8 is shown in Fig. 5. The trend in mass fraction of vapour along the axi-symmetric boundary is evident. It illustrates three distinct regions in the formation of the jet as noted by other researchers (e.g. Newman and Brzustowski, 1970). Firstly, the core jet, about 10 mm long, is the initial outflow of vapour into the atmosphere. The interaction between the vapour and the atmosphere means that the mixing is not instantaneous. In this region, the core jet is primarily made up of the issuing fluid. Secondly, the mixing layer where the vapour and air interact creates a gradient between the fully vapour core jet and the fully gas atmosphere. The properties of this region are dictated by the density ratio and the mixing law. The ambient atmosphere is the region not affected by the issuing jet and has conditions that are similar to atmospheric. The length of the jet is taken to be the mixing layer plus the core jet. In this case, its

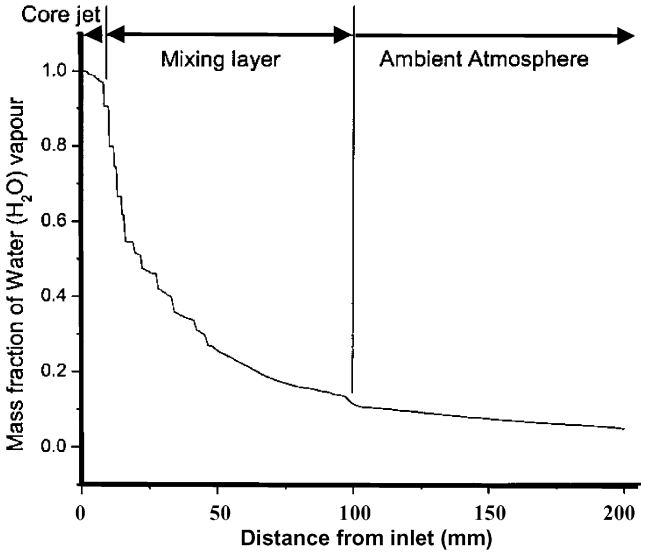

Fig. 5. Vapour mass fraction profile for the steady vapour jet.

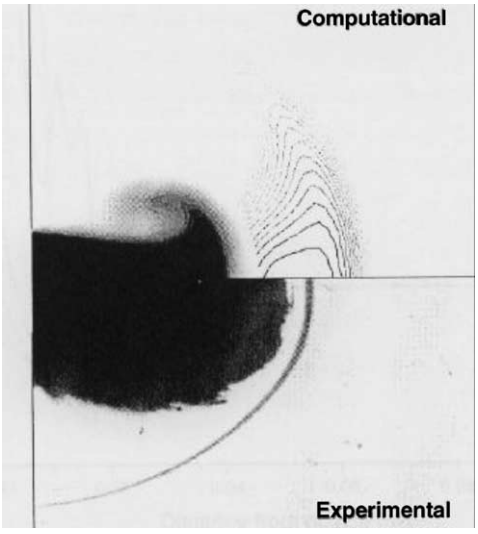

Fig. 7. Simulation–experiment comparison for the unsteady vapour jet.

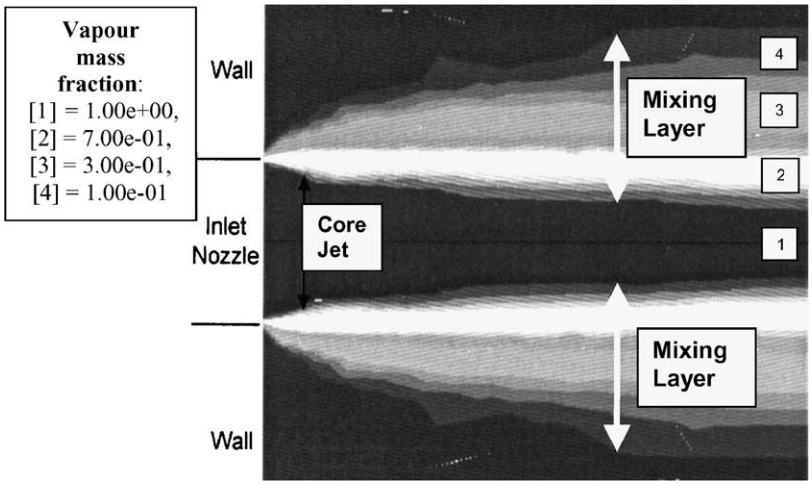

Fig. 6. Core jet and mixing layer mass fractions for the steady vapour jet.

length is due to the momentum of the liquid vapour at Mach 1.8. The mixing layer is important in dictating the shape and dynamics of the jet.

Fig. 6 illustrates the core jet and the distribution in the mixing layer. Immediately at the nozzle exit, the core jet has the same length scale as the nozzle diameter. As the jet moves in the axial direction, the mixing layer begins to form. The mixing gradient is initially quite steep, but plateaus to a constant value at about one third of the nozzle radius from the nozzle exit. As the core jet diameter decreases, the mixing layer profile increases. The jet is fully mixed when the core terminates.

4.1.2. Unsteady calculations

As the jet impinges upon the quiescent gaseous atmosphere, the air ahead of it is accelerated by the interaction. The air reaches supersonic speed very quickly and the shock wave is formed. In the computational model, the vapour jet must interact with the air domain in a similar manner. In unsteady calculations, the effect of the vapour influx from the inlet on the atmosphere is integrated over time. The fluid regime properties are calculated at each time step. The unsteady equations track the path of the jet head and hence predict its intensification and attenuation. The shock will dissipate completely at time approaching infinity, this being the steady state solution. Figs. 7 and 8 show typical solutions for the shock wave and the vapour mass fraction respectively. The computational shock is smeared over several cells. While further grid refinement could improve the shock sharpness, these are computationally expensive and the improvements in the understanding of the jet mixing are unlikely to be significant. Further study on this point is warranted in the future. Note that there is surprising similarity between the shock stand-off and jet shape for the simulated vapour jet and the liquid jet experiments.

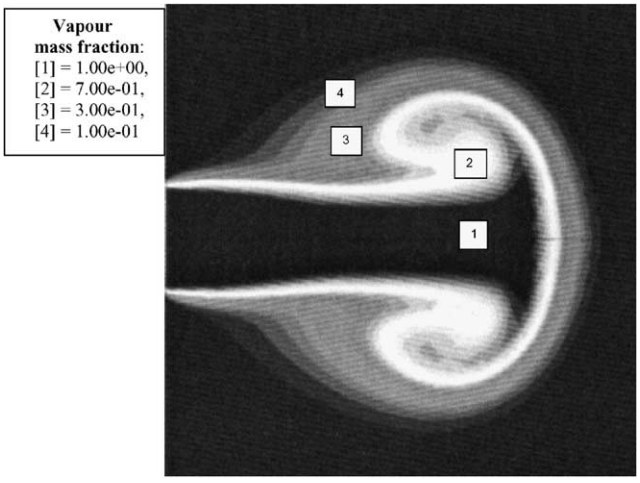

Fig. 8. Mass fraction at 100 μs for the for the unsteady vapour jet.

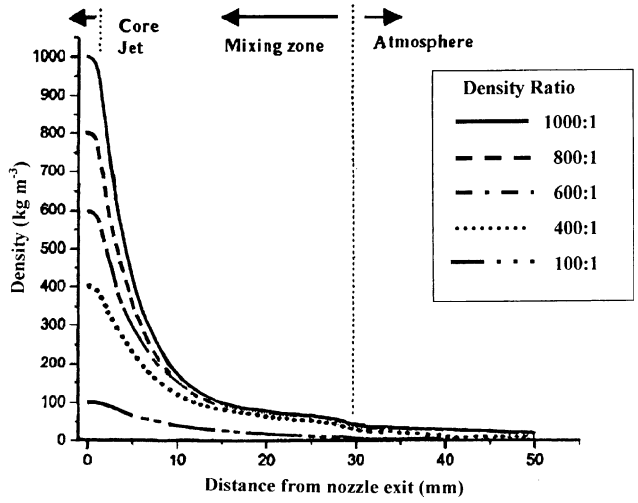

Fig. 9. Steady liquid jet mass fraction with density ratio variation.

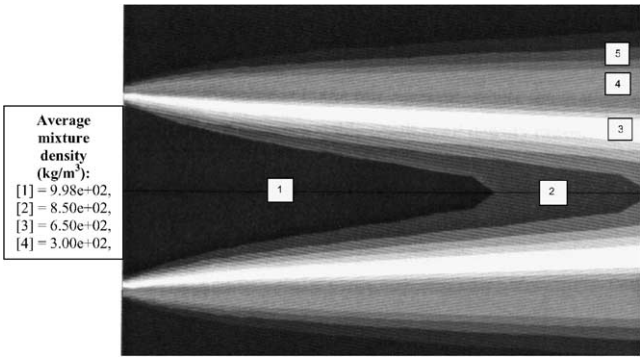

Fig. 10. Core jet and mixing layer mass fractions for the steady liquid jet.

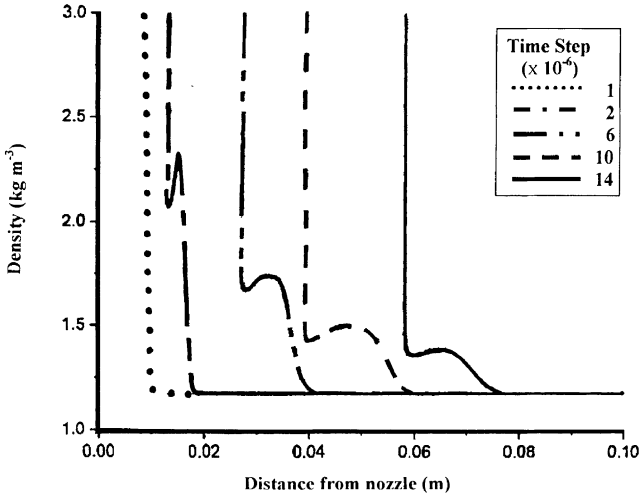

Fig. 11. Unsteady liquid jet: density along the jet axis.

4.2. The liquid jet

4.2.1. Steady state calculations

For a liquid Mach 1.8 jet, a steady state solution was computed for constant density of each species, the liquid density being set to 998 $kg\,m^{-3}$ with the N_2–O_2 mixture using the UDF approach for the gas density.

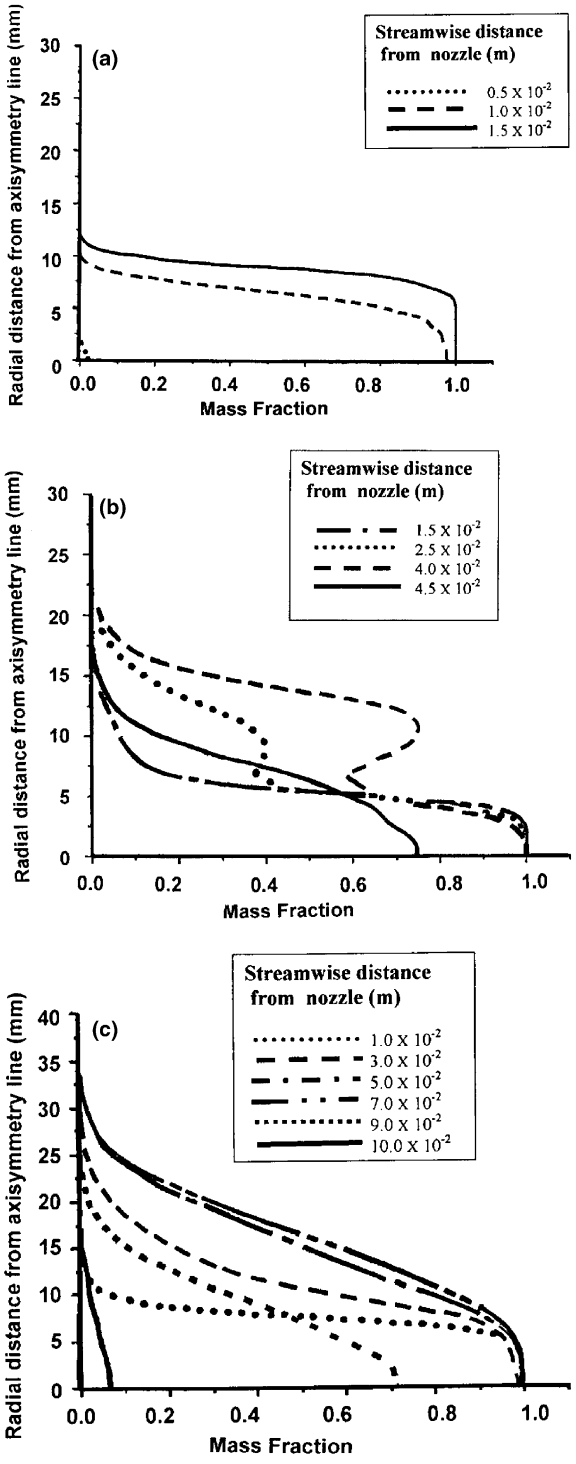

Fig. 12. Unsteady liquid jet: from top-radial mass fractions at 20, 120 and 700 μs.

Results for initial liquid density ratios from 2 to 1000 are shown on Fig. 9. As with the vapour jet, the core jet, mixing layer and atmosphere are clearly discernible although the lengths are shorter. For example, the intact core is now only a few millimetres long while the mixing layer extends to 30 mm. This is likely to be due to the jet diffusion properties remaining roughly constant while the turbulence in the shear layer increases substantially with the core density. A through-jet profile (Fig. 10) also illustrates these shorter lengths.

4.2.2. Unsteady calculations

Fig. 11 shows the evolving jet. Physically, the intermittent jet is attenuating and hence the shock shape is transient, evolving as the jet geometry and velocity change. Also, the interface between the liquid and the gas is not a solid wall. As the liquid jet is atomised, the core becomes increasingly porous so that air enters the mixing region in a similar manner to a quasi-porous medium. The jet head (that is, the air–liquid interface) is illustrated by the vertical line on Fig. 11. A mixing layer exists ahead of the interface but behind the shock. This reduces in density but increases in width as the time and hence distance from the nozzle increases. Mass concentrations at different radial positions can be seen on Fig. 12.

5. Conclusions

Supersonic liquid jets in the range from about $M = 1.8$ to $M = 5.6$ have been studied experimentally and with the use of a proprietary CFD code. In this paper, the focus is on jets at the lower end of this range as these may have a more immediate application. The CFD development has examined the shock structure ahead of the jet, and the mixing layer for jets emerging from the nozzle as either vapour or liquid. So far, the jet fluid considered has been water or water vapour. Considerable effort was required to obtain convergence in the simulation and user defined functions (UDFs) were helpful although not always applicable. As yet, the simulation includes the default models from the code for atomization and mixing. User developed models should allow an improved exploration of these effects in later work. However to date, the density and species concentrations in the mixing layer have been assessed and should provide useful data for combustion studies. In particular, these will help to provide information relevant to the ignitability and subsequent combustion of supersonic fuel jets.

As yet, the simulation includes the default models from the code for atomization and mixing. User developed models should allow an improved exploration of these effects in later work. However to date, the density

and species concentrations in the mixing layer have been assessed and should provide useful data for combustion studies. In particular, these will help to provide information relevant to the ignitability and subsequent combustion of supersonic fuel jets.

References

Ben-Dor, G., Britian, A., Elperin, T., Igra, O., Jaing, J.P., 1997. Experimental investigations of the interaction between weak shock waves and granular layer. Exp. Fluids 2 (2), 432–443.

Bloor, M.I.G., 1978. Hypersonic liquid jets. J. Fluid Mech. 84 (2), 375–384.

Field, J.E., Lesser, M.B., 1977. On the mechanics of high speed liquid jets. Proc. Royal Soc. London, Ser. A 357, 143–162.

Lian, Z.W., Reitz, R.D., 1993. The effect of vaporisation and gas compressibiltiy on liquid jet atomization. J. Atomization Spray 3, 249–264.

Nakahira, T., Komori, M., Nishida, N., Tsujimura, K., 1991. A study of shock wave generation around high pressure fuel spray in diesel engine. In: Takayama, K. (Ed.), ISSW18, Proceedings of the 18th International Shock Waves Symposium, vol. 2(5). Sendai, pp. 1271–1276.

Newman, J.A., Brzustowski, T.A., 1970. Break-up of a liquid jet in a high-pressure environment. AIAA J. 8 (2), 164–165.

Pianthong, K., Zakrzewski, S., Milton, B.E., Behnia, M., 2002. Supersonic liquid jets: their generation and shock wave characteristics. Shock Wave J. 11 (6), 457–466.

Pianthong, K., Zakrzewski, S., Behnia, M., Milton, B.E., 2003. Characteristics of impact driven supersonic liquid jets. Exp. Therm. Fluid Sci. 27, 589–598.

Reitz, R.D., Bracco, F.V., 1982. Mechanism of atomization of a liquid jet. Phys. Fluids 2 (5), 1730–1742.

Resnyansky, A.D., Milton, B.E., Romensky, E.I., 1997. A two-phase shock-wave model of hypervelocity liquid jet injection into air. In: JSME Centennial Grand Congress, International Conference on Fluid Engineering, Tokyo, 1997.

Shi, H.H., Takayama, K., 1995. Generation of high-speed liquid jets by high speed impact of a projectile. JSME Int. J., Ser. B 38, 181–190.

Shi, H.H., Takayama, K., 1999. Generation of hypersonic liquid fuel jets accompanying self-combustion. Shock Wave J. 9, 327–332.

Zakrzewski, S., Behnia, M., Milton, B.E., 2002. A blunt body analogy for bow shock characteristics in front of a supersonic liquid jet. In: Proceedings of the 2nd International Conference on Comp Fluid Dynamics, ICCFD2, Sydney, July, 2002.